Published in final edited form as:

J Vasc Surg. 2016 December ; 64(6): 1835–1846.e1. doi:10.1016/j.jvs.2015.09.052.

Establishment of a rat and guinea pig aortic interposition graft model reveals model specific patterns of intimal hyperplasia

Elaine K. Gregory, MD[a], **Janet M. Vercammen, AAS**[a], **Megan E. Flynn, MS**[a], and **Melina R. Kibbe, MD**[a,b]

[a]Division of Vascular Surgery, Feinberg School of Medicine, and Simpson Querrey Institute for Bionanotechnology, Northwestern University

[b]Division of Vascular Surgery, Feinberg School of Medicine, and the Jesse Brown Veterans Affairs Medical Center

Abstract

Objective—Although the aortic interposition bypass model has been widely used to evaluate biomaterials for bypass grafting, there is no comprehensive description of the procedure or of the distribution of intimal hyperplasia that results. The objectives of this study were to (1) review and summarize approaches of aortic interposition grafting in animal models, (2) determine the pertinent anatomy for this procedure, (3) validate this model in the rat and guinea pig, and (4) compare the distribution of intimal hyperplasia that develops in each species.

Methods—A literature search was performed in PubMed from 1980 to the present to analyze the use of anesthesia, anticoagulation, antiplatelet agents, graft material, suture, and anastomotic techniques. Using 10-week-old male Sprague-Dawley rats and Hartley guinea pigs, we established pertinent aortic anatomy, developed comparable models, and assessed complications for each model. At 30 days, the graft and associated aorta were explanted, intimal formation was assessed morphometrically, and cellularity was assessed via nuclear counting.

Results—We reviewed 30 articles and summarized the pertinent procedural findings. Upon establishing both animal models, key anatomic differences between the species that affect this model were noted. Guinea pigs have a much larger cecum, increased retroperitoneal fat, and lack the iliolumbar vessels compared with the rat. Surgical outcomes for the rat model included a 53%

Correspondence: Melina R. Kibbe, MD, Division of Vascular Surgery, 676 N St. Clair St, #650, Chicago, IL 60611 (mkibbe@nmh.org).

Author conflict of interest: none.

Additional material for this article may be found online at www.jvascsurg.org.

The editors and reviewers of this article have no relevant financial relationships to disclose per the JVS policy that requires reviewers to decline review of any manuscript for which they may have a conflict of interest.

Author Contributions: Conception and design: EG, MK
Analysis and interpretation: EG, JV, MF, MK
Data collection: EG, JV, MF
Writing the article: EG, JV, MF, MK
Critical revision of the article: EG, JV, MF, MK
Final approval of the article: EG, JV, MF, MK
Statistical analysis: EG, MK
Obtained funding: EG, MK
Overall responsibility: MK

technical success rate and a 32% technical error rate. Surgical outcomes for the guinea pig model included a 69% technical success rate and a 31% technical error rate. These two species demonstrated unique distribution of intimal hyperplasia at 30 days. Intimal hyperplasia in the rat model was greatest at two areas, the proximal graft ($54 \times 10^2/\mu m^2$; $P < .001$) and distal graft ($28 \times 10^2/\mu m^2$; $P < .04$), whereas the guinea pig model developed similar intimal hyperplasia throughout the graft ($45\text{-}51 \times 10^2/\mu m^2$; $P < .01$).

Conclusions—In this report, we summarize the literature on the aortic interposition graft model, present a detailed description of the anatomy and aortic interposition graft procedure in the rat and guinea pig, and describe a unique distribution of intimal formation that results in both species. This information will be helpful when designing studies to evaluate novel graft materials in the future.

Clinical Relevance—Peripheral arterial disease affects ~8.5 million Americans and can require open surgical bypass grafting. However, vein is often not suitable or available, and expanded polytetrafluoroethylene continues to have poor infrapopliteal patency rates, necessitating the development of alternative graft materials. Although the aortic interposition graft model has been widely used to investigate new materials, the literature lacks a comprehensive description of this model. This report summarizes current approaches of aortic interposition grafting described in the literature, validates an aortic interposition bypass model in the rat and guinea pig, and compares the pattern of intimal hyperplasia that results from each species.

Peripheral arterial disease (PAD) is associated with significant morbidity and mortality, affecting ~8.5 million Americans,[1] many of whom require open surgical revascularization. The saphenous vein remains the ideal conduit but is not suitable or available in one-third of patients, necessitating the use of expanded polytetrafluoroethylene (ePTFE) graft material.[2] However, infrapopliteal patency rates for ePTFE grafts remain poor, with only 30% patent at 2 years and 12% patent at 5 years.[3] Thus, alternative graft materials are needed and must be evaluated using appropriate animal models.[2]

Animal models have been used to evaluate alternative conduits. The appropriateness of using animal bypass models to pattern pathology seen in humans has been questioned because they exhibit prolonged patency rates.[4,5] These differences are related to species-specific factors, differences in flow conditions, and rates of endothelialization. However, anastomotic intimal hyperplasia is the pathophysiologic process responsible for the intimal formation that occurs in animal and human bypass grafts, thus making it a reasonable place to begin initial investigations of new therapies and approaches.

The aortic interposition bypass graft model has been used extensively to evaluate new graft materials. However, current literature lacks a comprehensive review of the anatomy, detailed description of the procedure, and description of the distribution of intimal hyperplasia that develops. In this study, we sought to establish and validate a small-animal aortic interposition bypass graft model in the rat and guinea pig to evaluate novel biomaterials. The objectives of this study were to (1) summarize current approaches of aortic interposition grafting, (2) compare the pertinent anatomy for the rat and guinea pig, (3) validate an aortic interposition bypass model in the rat and guinea pig, and (4) evaluate and compare the pattern of intimal hyperplasia that results in each species.

Methods

All animal procedures in this study were performed in accordance with the *Guide for the Care and Use of Laboratory Animals* published by the National Institutes of Health (NIH Publication 85-23, 1996) and were approved by the Northwestern University Animal Care and Use Committee.

Literature search

Details of the literature search are available in the Supplementary Methods (online only)

Surgical procedure for establishment of the animal models

Details of the surgical procedure are available in the Supplementary Methods (online only).

Presurgical setup, positioning, and anesthetic management

Fig 1 depicts the surgical field and equipment, and Fig 2 depicts the surgical instrument setup. Table I summarizes all medications used, including species-specific dosing and indication.[6-11] For the rat model, 10-week-old male Sprague-Dawley rats, weighing 350 to 400 g, were induced with 5% isoflurane and then maintained on 1.5% to 2.0% isoflurane. Preoperative medications included carprofen (5 mg/kg subcutaneously [SQ]) for analgesia and atropine (0.01 mg/kg SQ) to reduce airway secretions. For the guinea pig model, 10-week-old Hartley guinea pigs, weighing 450 to 500 g, were induced with 5% isoflurane and maintained on 1.5% to 2.0% isoflurane. Preoperative medications included carprofen (3 mg/kg SQ) and atropine (0.1 mg/kg SQ). All animals received antibiotic prophylaxis with enrofloxacin (5 mg/kg SQ). Guinea pigs are prone to gastroduodenal ulceration and also received ranitidine (5 mg/kg) as prophylaxis.[12]

Abdominal exploration, aortic exposure, and anatomic differences

Fig 3 demonstrates the surgical positioning of the animals. Temperature was maintained in all animals using a warming pad (Fig 1). The abdomen was sterilely prepared and draped (Fig 4) and opened using scissors, extending cranially to 5 mm below the xiphoid process and caudally to above the bladder (Fig 4, A and F). The cecum and small bowel were eviscerated, wrapped in gauze, and retracted superiorly (Fig 4, B and G). Retractors were placed in the right and left upper and lower quadrants, exposing the retroperitoneum (Fig 4, C and H). The small bowel retroperitoneal attachments were divided, and the small bowel was retracted to the right upper quadrant. A dissecting microscope (Leica, Buffalo Grove, Ill) was used to open the retroperitoneum.

The aortic diameters of the rat and guinea pig have been reported to be similar, ~1.2 mm and 1.1 mm, respectively,[13] but other anatomic differences were noted (Fig 5). The guinea pig lacks iliolumbar arteries and veins, but both species have lumbar arteries and veins. The lumbar arteries in the rat arise from the dorsal surface of the aorta, whereas in the guinea pig they have a posterolateral orientation. In addition, the spermatic arteries and left renal vein are difficult to visualize in the guinea pig due to increased retroperitoneal fat. Lastly, the cecum is much larger in the guinea pig compared with the rat (Fig 4, B and G). Fig 5, B

depicts a double-barrel inferior vena cava, an anatomic variant more frequently encountered in the guinea pig.

After the large left iliolumbar vein was exposed in the rat (Fig 4, D), the dissection was carried cranially to expose the spermatic artery and left renal vein. Approximately 1.5 cm of the abdominal aorta was mobilized from the spermatic arteries to the aortic bifurcation. The left and right iliolumbar and proximal lumbar arteries in the rat and the lumbar arteries in the guinea pig were ligated (Fig 4, E and J). Heparin (rat: 100 U/kg; guinea pig: 400 U/kg SQ) was administered 20 minutes before aortic cross-clamping.

Creation of the anastomosis and restoration of blood flow

Fig 6 depicts details of the anastomosis, which was created with 12 interrupted 9-0 nylon sutures. The distal clamp was applied at the iliac bifurcation, and the proximal clamp was applied close to the spermatic arteries. With the approximator clamp (Synovis, Birmingham, Ala) in place to reduce tension, the aorta was transected 2 to 4 mm below the left iliolumbar artery (Fig 6, B). After the approximator clamp was removed, the aorta was irrigated with heparinized saline, and Visibility Background Material (Synovis) was placed behind the aorta and approximator clamp to protect the underlying structures while suturing (Fig 6, B).

Loose adventitia was removed from the proximal end of the aorta, and the artery was dilated with 45° angled forceps. The A-frame approximator clamp was applied to the aorta and ePTFE graft (1.53 mm, IND 25 μm, wall thickness 100 μm; Zeus, Orangeburg, SC). Stay sutures with 9-0 nylon (BV130 needle; Suture Express, Lenexa, KS) were placed at the 3 and 9 o'clock positions and secured to the goal posts of the approximator clamp (Fig 6, C). A suture was placed at 12 o'clock (Fig 6, D), after which the approximator clamp was rotated 180° counterclockwise, exposing the posterior wall (Fig 6, E) to place a suture at 6 o'clock. Two additional stitches were placed in each of the four quadrants (Fig 6, E-I). The distal anastomosis was constructed similarly; however, the last suture placed anteriorly was not tied to permit clearance of air and debris proximally and distally. After flushing with heparinized saline, the remaining suture was tied, and oxidized regenerated cellulose (Surgicel; Suture Express) was placed over the anastomoses for 2 to 3 minutes, allowing for hemostasis of the suture line. Additional sutures were added judiciously, with care not to narrow the anastomosis. Patency was confirmed by a pulse in the distal aorta and by reperfusion of the lower extremities. The urinary bladder was gently decompressed manually before the bowel was returned to the peritoneal cavity. The rectus abdominis muscle and skin were closed separately with a running 4-0 nylon suture.

Postoperative care

Postoperative care is described in the Supplementary Methods (online only).

Morbidity and mortality assessment

Six complications were recorded: early graft thrombosis (<24 hours), late graft thrombosis (>24 hours), hemorrhage, technical complications, bowel and bladder complications, and failure to thrive. Technical complications were subcategorized as graft and artery tears, misplaced stitched, anesthesia, and insufficient arterial length.

Harvesting of specimens

At 1 month, animals were anesthetized as previously described and euthanized by bilateral thoracotomy. The graft and 5 mm of native aorta proximal and distal to the anastomoses were harvested after in situ perfusion-fixation with phosphate buffered saline (500 mL) and 2% paraformaldehyde (500 mL) through the left ventricle. The specimen was divided into proximal and distal segments, frozen in optimal cutting temperature compound using liquid nitrogen, and cut into 5-μm sections. Five to six equally spaced sections from six regions were stained with hematoxylin and eosin. The six regions included the proximal artery, proximal graft, proximal midgraft, distal midgraft, distal graft, and distal artery (Fig 7, A).

Morphometric analysis and assessment of intimal cellularity

This information is available in the Supplementary Methods (online only).

Statistical analysis

Statistical analysis is described in the Supplementary Methods (online only).

Results

Literature search

We identified 37 articles using the search terms specified. Seven articles were excluded: 3 were in mouse or rabbit, 1 described an anastomotic technique without sutures, 1 procedure was part of pancreatic transplant, and 2 were from the same author with similar methods. The remaining 30 articles used different species of rats, inserting the grafts at the abdominal aorta. These were reviewed and the approaches are summarized in Table II.[14-43] Most of the studies used an inhalational anesthetic, such as isoflurane (14 of 30), followed by ketamine/xylazine (7 of 30) and pentobarbital (8 of 30). Twelve studies used heparin, and six used intravenous heparin. Antiplatelet agents were described in two studies.

Regarding the aortic dissection, two studies described vessels ligated. Nine studies specified the method of aortic transection. Two studies used a beveled transection, and nine used a perpendicular transection with the removal of 3 to 15 mm of aorta. The diameter of the prosthetic grafts used ranged from 1 to 2 mm. Twenty studies used a graft length of 10 mm. Regarding the anastomosis, 11 studies used 10-0 nylon, 7 used 9-0 nylon, and 3 used 10-0 polypropylene sutures. Concerning stitch type and number of stitches used, 15 studies described the type of stitch as continuous vs interrupted, and four studies described the number stitches used ranging from 5 to 16.

With respect to the geometry of the anastomosis, of the 25 studies that described the type of anastomosis used, 23 were end-to-end, and only one study described the approach to fashion the anastomosis. Concerning duration of implantation, 26 studies described implantation times >2 weeks and ranging up to 52 weeks. Although 14 studies evaluated intimal hyperplasia, only five specified the areas investigated.

Surgical care and anesthesia

In the rat model, we used isoflurane, carprofen, atropine, and heparin (100 U/kg). In the guinea pig model, we initially used buprenorphine for analgesia, but it resulted in increased periods of anorexia, so carprofen was used instead. Despite increased intake, the guinea pig continued to exhibit failure to thrive postoperatively. Necropsy by our veterinarian staff early in the study revealed evidence of gastroduodenal ulcer formation, so ranitidine was added to the guinea pig's regimen for prophylaxis. To address increased early thrombosis rates noted in the guinea pigs compared with the rats, heparin was increased incrementally to 400 U/kg.

Procedural approach

In developing our model we focused on five considerations: (1) implantation location, (2) graft length, (3) suture size, (4) type of aortic transection, and (5) anastomotic technique. We found the ideal location for implantation was 2 to 4 mm below the left iliolumbar artery, cranial to the right iliolumbar artery. We evaluated nylon suture sized 8-0 to 10-0 and found 9-0 suture was optimal for visualization and handling. We evaluated perpendicular vs beveled transections of the aorta, and although a beveled transection decreased the incidence of back-walled stitches, it increased graft-to-artery size mismatch, so a perpendicular transection was used. We also evaluated aortic transection, with and without removal of 10 mm of native aorta, and found that transection alone resulted in the least amount of anastomotic tension. Lastly, we evaluated different anastomotic techniques, including interrupted vs continuous sutures and with and without the use of an approximator clamp. In our hands, interrupted sutures with the use of the A-frame approximator clamp resulted in superior approximation of the anastomosis.

Surgical outcomes for the rat

We used 32 rats to establish the aortic interposition graft model. Of these, 17 animals recovered from anesthesia (53%), with 14 surviving 24 hours (44%) and 13 surviving to 30 days (41%). Complications included early graft thrombosis in 4 (13%), late graft thrombosis in 1 (3%), hemorrhage in 4 (13%), and technical errors in 10 (32%). Technical errors included 3 graft tears, 4 back-walled stitches, and 3 grafts with excessive anastomotic tension.

Surgical outcomes for the guinea pig

We used 35 guinea pigs to establish the aortic interposition graft model. Of these, 24 recovered from anesthesia (69%), with 22 surviving 24 hours (63%), and 8 surviving 30 days (23%). Complications included early graft thrombosis in 10 (29%), late graft thrombosis in 1, (3%), hematuria in 1 (3%), failure to thrive in 2 (6%), and technical errors in 11 (31%). Technical errors included 3 graft tears, 2 back-walled stitches, 3 anesthetic deaths, and 3 grafts with excessive anastomotic tension.

Intimal formation and nuclear density

Intimal area varied widely at the six locations analyzed (Fig 7, B and C). In the rat, intimal formation was greatest at the proximal graft ($54 \times 10^2/\mu m^2$; $P < .001$), followed by the distal graft ($28 \times 10^2/\mu m^2$; $P < .04$). Mean intimal nuclear density was 1.7 nulcei/μm^2 at the

proximal graft and 1.4 nulcei/μm^2 at the distal graft. In the guinea pig, intimal formation developed along the entire length of the graft and ranged from 45 to 51 × 10^2/μm^2 ($P < .01$) throughout the graft. Mean intimal nuclear density was 2.1 nulcei/μm^2 at the proximal graft and 1.5 nuclei/μm^2 at the distal graft.

Comparing the degree of intimal formation between the species, we found that maximum intimal formation at any given region was similar between the two animal models, but overall, the guinea pig formed more total intimal hyperplasia throughout the graft than the rat (194 × 10^2 vs 107 × 10^2/μm^2, respectively; $P < .001$). Comparing mean nuclear density between the species, the guinea pig exhibited more intimal cellularity at the proximal graft than the rat ($P < .01$). Mean intimal cellularity was similar between the species at the distal graft.

Discussion

In this study, we reviewed and summarized the existing approaches to aortic interposition grafting. We established the aortic anatomy in the rat and guinea pig, documenting key anatomic differences and highlighting landmarks for performing this procedure. We also evaluated the anesthetics, anticoagulation, antiplatelet agents, and details of the approaches used in the literature, including conduit length, suture type, method of aortic transection, and the anastomotic techniques. To our knowledge, this is the first work to describe this model in the guinea pig and to analyze the distribution of intimal hyperplasia that develops throughout the entire specimen, revealing a unique pattern of intimal formation for each species.

Although the rat and guinea pig models both exhibited comparable rates of recovery from anesthesia and technical errors, the 30-day survival rates were higher in the rats. We attribute this to increased postoperative complications in the guinea pig, including early and late graft thrombosis, urinary retention, and failure to thrive. The most striking difference was a twofold increase in the early graft thrombosis rate, which required increased heparin administration in the guinea pig model. Differences in the coagulation cascade and platelet activation between rats and guinea pigs may also explain this increased heparin requirement. The prothrombin time is similar in rats (15.9 seconds) and guinea pigs (16.8 seconds) but is considerably shorter than the prothrombin time in humans (35.9 seconds).

The thrombin times in rats (66 seconds), guinea pigs (35.2 seconds), and humans (15.4 seconds) are also very different.[44,45] The shorter thrombin time in the guinea pig may explain the increased thrombosis rate observed. Although not the primary site of action of heparin, prolongation of thrombin time has been observed with high doses of unfractionated heparin and might explain why such a high dose of heparin was required to see an effect on early thrombosis rates in the guinea pig.

Comparing our model with those in the published literature with respect to anesthesia and preoperative medications, we found that isoflurane offered the best anesthetic control. Heparin was needed to decrease early thrombosis, but antiplatelets agents were not required. Although most studies described inserting the graft below the renal arteries and above the iliac bifurcation, we identified that the optimal level of aortic transection and graft insertion

was 2 to 4 mm below the left iliolumbar artery. Transection of the aorta more cranially hindered visualization of the proximal aorta due to variable aortic retraction, whereas transection more caudally hindered mobility of the distal aorta due to tethering at the iliacs. Most of the studies used a perpendicular aortic transection, but two studies described a beveled transection.[26,29] We evaluated beveled transection of the artery, with and without beveled transections of the graft, to improve graft and artery size matching, but in our hands found that perpendicular transection of the artery and graft resulted in more consistent size matching.

Unlike the nine studies that removed variable amounts of aorta on transection,[14,19,26,29,31,38,40,42,43] for consistency between animals and to prevent any anastomotic tension, we transected the aorta without removing any native artery. With respect to details of the anastomosis, most of the studies used 10-0 nylon suture, but we found 9-0 was better visualized than 10-0 and was more manageable than 8-0 in fashioning the anastomosis. Similar to 11 of the prior studies,[14,19,25,26,29-31,37,41,42] we used interrupted sutures and found that 12 interrupted sutures were sufficient to fashion each anastomosis.

Of the 30 studies reviewed, only Enomoto et al[31] discussed details of the anastomotic approach. Thus, most of our approach was established from the available microsurgical literature. Using the same technique of triangulation initially described by Carrel,[46] MacDonald[47] recommends placing stay sutures at the 10 and 2 o'clock positions to fashion the anastomosis to prevent coaptation of the lumen, whereas Yonekawa et al[48] recommend placing stay sutures on diagonally opposite sides of the anastomotic plane. Similar to Yonekawa et al, Yagi et al[38] describes sutures 180° apart, at the 12 and 6 o'clock positions, which necessitates a left/right wall approach, precluding the use of the approximator clamp and requiring repetitive manipulation of stay sutures to assess alignment. Repetitive manipulation of the stay sutures increased graft needle holes, confounding the evaluation of hemostasis once flow was restored. Alternatively, we placed these at the 9 and 3 o'clock positions, approximating the sides of the artery and graft. This facilitated the use of an A-frame approximator clamp, which allowed for securing of the stay sutures, and the use of a posterior/anterior wall approach as described by Enomoto et al.[31]

Several details regarding anastomotic creation highlighted in the microsurgical literature are worth noting. Most importantly, to restore blood flow, the cross-clamps should be removed gradually to permit resolution of bleeding from the suture line and needle holes in the graft. Yonekawa et al[48] recommend clamping the distal clip transiently and waiting ~1 to 2 minutes for platelet aggregation and sealing of the suture line. This is especially crucial for prosthetic grafts, because unlike arterial and venous conduits, prosthetic materials lack an elastic component to limit bleeding from needle holes. As did Yonekawa et al,[48] we recommend placing additional sutures sparingly because this can result in occlusion of the anastomosis.[49] Another key point is that surgeon's knots give the most control in the approximation of the artery and conduit.[48] In addition, when prosthetic graft is used, this decreases the extension of needle holes onto the graft material. Lastly, use of visibility background material to protect the vena cava and other large veins from desiccation or injury and the utility of an A-frame approximator clamp for approximation of the anastomosis were helpful suggestions from the microsurgical literature.

Among the published literature, comparison of the amount of intimal hyperplasia and its distribution throughout the graft was limited due to differences in the methods used and the data analyzed and recorded. Intimal formation differs according to the conduit material, time of implantation, and the anastomotic technique. Furthermore, only 14 of the 30 articles quantitated some measure of intimal hyperplasia, and only three used ePTFE. Jeschke et al[20] had a comparable model and specified the location investigated, but this was expressed in intimal thickness not intimal area. Similarly, none of these studies investigated the distribution of intimal hyperplasia that developed throughout the entire graft.

One of the most interesting findings of this study was the different pattern of intimal formation observed between the two species. The literature suggests that anastomotic intimal hyperplasia is responsible for the intimal formation that develops in animal models and humans, and various factors can affect the amount and distribution of the neointima that develops. Zilla et al[5] summarized the major factors influencing the development of anastomotic intimal hyperplasia, such as flow conditions, shear stress, graft material, and endothelialization, and highlighted key factors that differ between human and small-animal experimental models. Because graft configuration and graft material were similar between the two species in our experiments, endothelialization remains a potential etiology for the differences observed between the two species.

Transanastomotic endothelialization is the process that establishes endothelialization of the graft material. The three most important factors affecting the rate of transanastomotic endothelialization include conduit length, species, and age.[5] Because conduit length and age were controlled for between the rat and guinea pig, the only remaining factor influencing endothelialization is species. Thus, we hypothesize that the different patterns of intimal hyperplasia observed between the rat and guinea pig may be due to different rates of endothelialization between the species. Further study will be necessary to definitively prove this hypothesis.

Because we observed different patterns of intimal formation between the species, we investigated whether there were differences in the cellularity of the intimal tissue that develop between these two species. We did observe an increase in nuclear density at the proximal graft in the guinea pig compared with the rat, but the nuclear density at the distal graft for both species was similar. Whether the etiology of this increased cellularity in the guinea pig is due to increased proliferation of certain cell types or increased cellular infiltration is unclear. Further study will be required to delineate these differences.

There are admittedly some weaknesses in our study. Although we have compiled a comprehensive review of this procedure, our final model was based on the experience of one surgeon. As such, this work is not intended to replace formal microsurgical instruction. We have cited the reports we used to establish proper microsurgical techniques.[47,48] In addition, we refer the reader to review the videos from the Columbia Orthopedics Microsurgery Research & Training Laboratory at Columbia University Medical Center (http://microsurg.hs.columbia.edu/MicrosurgeryVideos.html). Lastly, although we clearly demonstrated different patterns of intimal hyperplasia in these two models, we did not

provide a mechanism for these differences because that was far beyond the scope of this report.

Conclusions

In evaluating novel technologies, using models that best simulate the human clinical scenario is of utmost importance. Animal models have proven invaluable tools to evaluate novel technologies. In this report, we have reviewed and summarized the methods of aortic interposition bypass models in the literature and illustrated and compared the rat and guinea pig abdominal aorta anatomy, highlighting key differences. We have also presented a comprehensive description of aortic interposition grafting in the rat and validated a novel model in the guinea pig. Lastly, we characterized the resulting intimal formation that developed throughout the entire graft, establishing that a unique pattern develops in each species. These data will be helpful when designing studies to evaluate novel graft materials in the future.

Supplementary Material

Refer to Web version on PubMed Central for supplementary material.

Acknowledgments

This work was supported by funding from the National Institutes of Health (T32-HL0-94293-01 and 1-F32-HL1-14255-01A1 to E.G.), the American Heart Association (No. 12POST12150050 to E.G); the Society for Vascular Surgery Foundation to M.K.; Northwestern Memorial Foundation Collaborative Development Initiative, Center for Limb Preservation, Bluhm Cardiovascular Institute; and the Veterans Affairs Merit Award Program (1 I01 BX002282-01A1 to M.K.).

References

1. Mozaffarian D, Benjamin EJ, Go AS, Arnett DK, Blaha MJ, Cushman M, et al. Executive summary: heart disease and stroke statistics-2015 update: a report from the American Heart Association. Circulation. 2015; 131:434–41.
2. Park KM, Kim YW, Yang SS, Kim DI. Comparisons between prosthetic vascular graft and saphenous vein graft in femoro-popliteal bypass. Ann Surg Treat Res. 2014; 87:35–40. [PubMed: 25025025]
3. Eagleton MJ, Ouriel K, Shortell C, Green RM. Femoral-infrapopliteal bypass with prosthetic grafts. Surgery. 1999; 126:759–64. [PubMed: 10520926]
4. Byrom MJ, Bannon PG, White GH, Ng MK. Animal models for the assessment of novel vascular conduits. J Vasc Surg. 2010; 52:176–95. [PubMed: 20299181]
5. Zilla P, Bezuidenhout D, Human P. Prosthetic vascular grafts: wrong models, wrong questions and no healing. Biomaterials. 2007; 28:5009–27. [PubMed: 17688939]
6. Canadian Council on Animal Care. Guide to the care and used of experimental animalsVol 1. Ottawa, ON: Canadian Council on Animal Care; 1980.
7. Hawke, C.; Leary, SL.; Morris, TH. Formulary for laboratory animals. 3rd. Ames, IA: Wiley-Blackwell; 2005.
8. Liles J, Flecknell PA. The influence of buprenorphine or bupivacaine on the post-operative effects of laparotomy and bile-duct ligation in rats. Lab Anim. 1993; 27:374–80. [PubMed: 8277712]
9. Carpenter, J. Exotic animal formulary. St. Louis, MO: Saunders; 2005.
10. Melby, E.; Altman, NH. Handbook of laboratory animal science. Boca Raton, FL: CRC Press; 1974.

11. Flecknell, P. Laboratory animal anaesthesia: a practical introduction for research workers and technicians. 2nd. St. Louis, MO: Elsevier; 1996.
12. Jervis HR, Sheahan DG, Sprinz H. Acute duodenal ulcerations in the guinea pig due to fasting. Delineation of experimental model. Lab Invest. 1973; 28:501–13. [PubMed: 4703852]
13. Medeiros de Mello J, Orsi AM, Padovani CR, Matheus SM, Eleutério ML. Structure of the aortic wall in the guinea pig and rat. Braz J Morphol Sci. 2004; 21:35–8.
14. Yeh HS, Keller JT, Brackett KA, Frank E, Tew JM Jr. Human umbilical artery for microvascular grafting. Experimental study in the rat. J Neurosurg. 1984; 61:737–42. [PubMed: 6470785]
15. Ribbe EB, Holmin T, Lowenhielm PC. Microvascular polytetra-fluoroethylene (Gore-Tex) grafts in the infrarenal rat aorta. Microsurgery. 1987; 8:48–53. [PubMed: 3626823]
16. Lepidi S, Sterpetti AV, Cucina A, Randone B, Palumbo R, Patrizi AL, et al. The degree of porosity influences the release of growth factors by healing polytetrafluoroethylene (PTFE) grafts. Eur J Vasc Endovasc Surg. 1996; 11:36–41. [PubMed: 8564484]
17. Randone B, Sterpetti AV, Stipa F, Proietti P, Aromatario C, Guglielmi MB, et al. Growth factors and myointimal hyperplasia in experimental aortic allografts. Eur J Vasc Endovasc Surg. 1997; 13:66–71. [PubMed: 9046917]
18. Poston RS, Tran KP, Mann MJ, Hoyt EG, Dzau VJ, Robbins RC. Prevention of ischemically induced neointimal hyperplasia using ex vivo antisense oligodeoxynucleotides. J Heart Lung Transplant. 1998; 17:349–55. [PubMed: 9588579]
19. Dardik A, Liu A, Ballermann BJ. Chronic in vitro shear stress stimulates endothelial cell retention on prosthetic vascular grafts and reduces subsequent in vivo neointimal thickness. J Vasc Surg. 1999; 29:157–67. [PubMed: 9882800]
20. Jeschke MG, Hermanutz V, Wolf SE, Koveker GB. Polyurethane vascular prostheses decreases neointimal formation compared with expanded polytetrafluoroethylene. J Vasc Surg. 1999; 29:168–76. [PubMed: 9882801]
21. Sterpetti AV, Cucina A, Randone B, Guglielmi MB, Fragale A, Cavallaro A. Increased production of cytokines and growth factors by aortic allografts: a possible explanation for myointimal hyperplasia formation. Eur Surg Res. 1999; 31:297–304. [PubMed: 10449988]
22. Andriambeloson E, Bigaud M, Schraa EO, Kobel T, Lobstein V, Pally C, et al. Endothelial dysfunction and denudation in rat aortic allografts. Arterioscler Thromb Vasc Biol. 2001; 21:67–73. [PubMed: 11145935]
23. Johnson P, Carpenter M, Hirsch G, Lee T. Recipient cells form the intimal proliferative lesion in the rat aortic model of allograft arteriosclerosis. Am J Transplant. 2002; 2:207–14. [PubMed: 12096782]
24. Kidd KR, Patula VB, Williams SK. Accelerated endothelialization of interpositional 1-mm vascular grafts. J Surg Res. 2003; 113:234–42. [PubMed: 12957135]
25. Yamamoto K, Onoda K, Sawada Y, Fujinaga K, Imanaka-Yoshida K, Yoshida T, et al. Locally applied cilostazol suppresses neointimal hyperplasia and medial thickening in a vein graft model. Ann Thorac Cardiovasc Surg. 2007; 13:322–30. [PubMed: 17954989]
26. Cikirikcioglu M, Pektok E, Cikirikcioglu YB, Osorio-da Cruz S, Tille JC, Kalangos A, et al. Matching the diameter of ePTFE bypass prosthesis with a native artery improves neoendothelialization. Eur Surg Res. 2008; 40:333–40. [PubMed: 18303269]
27. Thaunat O, Louedec L, Graff-Dubois S, Dai J, Groyer E, Yacoub-Youssef H, et al. Antiangiogenic treatment prevents adventitial constrictive remodeling in graft arteriosclerosis. Transplantation. 2008; 85:281–9. [PubMed: 18212634]
28. Gui L, Muto A, Chan SA, Breuer CK, Niklason LE. Development of decellularized human umbilical arteries as small-diameter vascular grafts. Tissue Eng Part A. 2009; 15:2665–76. [PubMed: 19207043]
29. Pektok E, Cikirikcioglu M, Tille JC, Kalangos A, Walpoth BH. Alcohol pretreatment of small-diameter expanded polytetrafluoro-ethylene grafts: quantitative analysis of graft healing characteristics in the rat abdominal aorta interposition model. Artif Organs. 2009; 33:532–7. [PubMed: 19566729]

30. Nieponice A, Soletti L, Guan J, Hong Y, Gharaibeh B, Maul TM, et al. In vivo assessment of a tissue-engineered vascular graft combining a biodegradable elastomeric scaffold and muscle-derived stem cells in a rat model. Tissue Eng Part A. 2010; 16:1215–23. [PubMed: 19895206]
31. Enomoto S, Sumi M, Kajimoto K, Nakazawa Y, Takahashi R, Takabayashi C, et al. Long-term patency of small-diameter vascular graft made from fibroin, a silk-based biodegradable material. J Vasc Surg. 2010; 51:155–64. [PubMed: 19954921]
32. Chen Z, Hasegawa T, Tanaka A, Okita Y, Okada K. Pioglitazone preserves vein graft integrity in a rat aortic interposition model. J Thorac Cardiovasc Surg. 2010; 140:408–16.e401. [PubMed: 20189191]
33. Ladhoff J, Fleischer B, Hara Y, Volk HD, Seifert M. Immune privilege of endothelial cells differentiated from endothelial progenitor cells. Cardiovasc Res. 2010; 88:121–9. [PubMed: 20388638]
34. Thaunat O, Graff-Dubois S, Brouard S, Gautreau C, Varthaman A, Fabien N, et al. Immune responses elicited in tertiary lymphoid tissues display distinctive features. PloS One. 2010; 5:e11398. [PubMed: 20613979]
35. He W, Nieponice A, Soletti L, Hong Y, Gharaibeh B, Crisan M, et al. Pericyte-based human tissue engineered vascular grafts. Biomaterials. 2010; 31:8235–44. [PubMed: 20684982]
36. Nakao A, Huang CS, Stolz DB, Wang Y, Franks JM, Tochigi N, et al. Ex vivo carbon monoxide delivery inhibits intimal hyperplasia in arterialized vein grafts. Cardiovasc Res. 2011; 89:457–63. [PubMed: 20851811]
37. Soletti L, Nieponice A, Hong Y, Ye SH, Stankus JJ, Wagner WR, et al. In vivo performance of a phospholipid-coated bioerodable elastomeric graft for small-diameter vascular applications. J Biomed Mater Res A. 2011; 96:436–48. [PubMed: 21171163]
38. Yagi T, Sato M, Nakazawa Y, Tanaka K, Sata M, Itoh K, et al. Preparation of double-raschel knitted silk vascular grafts and evaluation of short-term function in a rat abdominal aorta. J Artif Organs. 2011; 14:89–99. [PubMed: 21344164]
39. Sun Q, Kawamura T, Masutani K, Peng X, Sun Q, Stolz DB, et al. Oral intake of hydrogen-rich water inhibits intimal hyperplasia in arterialized vein grafts in rats. Cardiovasc Res. 2012; 94:144–53. [PubMed: 22287575]
40. Wu W, Allen RA, Wang Y. Fast-degrading elastomer enables rapid remodeling of a cell-free synthetic graft into a neoartery. Nat Med. 2012; 18:1148–53. [PubMed: 22729285]
41. Pennel T, Zilla P, Bezuidenhout D. Differentiating transmural from transanastomotic prosthetic graft endothelialization through an isolation loop-graft model. J Vasc Surg. 2013; 58:1053–61. [PubMed: 23541549]
42. Kumar VA, Caves JM, Haller CA, Dai E, Liu L, Grainger S, et al. Acellular vascular grafts generated from collagen and elastin analogs. Acta Biomater. 2013; 9:8067–74. [PubMed: 23743129]
43. DallOlmo L, Zanusso I, Di Liddo R, Chioato T, Bertalot T, Guidi E, et al. Blood vessel-derived acellular matrix for vascular graft application. Biomed Res Int. 2014; 2014:685426. [PubMed: 25136610]
44. Kaspareit J, Messow C, Edel J. Blood coagulation studies in guinea pigs (Cavia porcellus). Lab Anim. 1988; 22:206–11. [PubMed: 3172700]
45. Lewis JH, Van Thiel DH, Hasiba U, Spero JA, Gavaler J. Comparative hematology and coagulation: studies on rodentia (rats). Comp Biochem Physiol A Comp Physiol. 1985; 82:211–5. [PubMed: 2864203]
46. Sade RM. Transplantation at 100 years: Alexis Carrel, pioneer surgeon. Ann Thorac Surg. 2005; 80:2415–8. [PubMed: 16305931]
47. MacDonald JD. Learning to perform microvascular anastomosis. Skull Base. 2005; 15:229–40. [PubMed: 16175232]
48. Yonekawa Y, Frick R, Roth P, Taub E, Imhof H. Laboratory training in microsurgical techniques and microvascular anastomosis. Oper Tech Neurosurg. 1999; 2:149–58.
49. Yap, L.; Butler, CE. Principles of microsurgery. In: Thorne, C., editor. Grabb and Smith's plastic surgery. 6th. Philadelphia, PA: Lippincott Williams & Wilkins; 2007. p. 66-72.

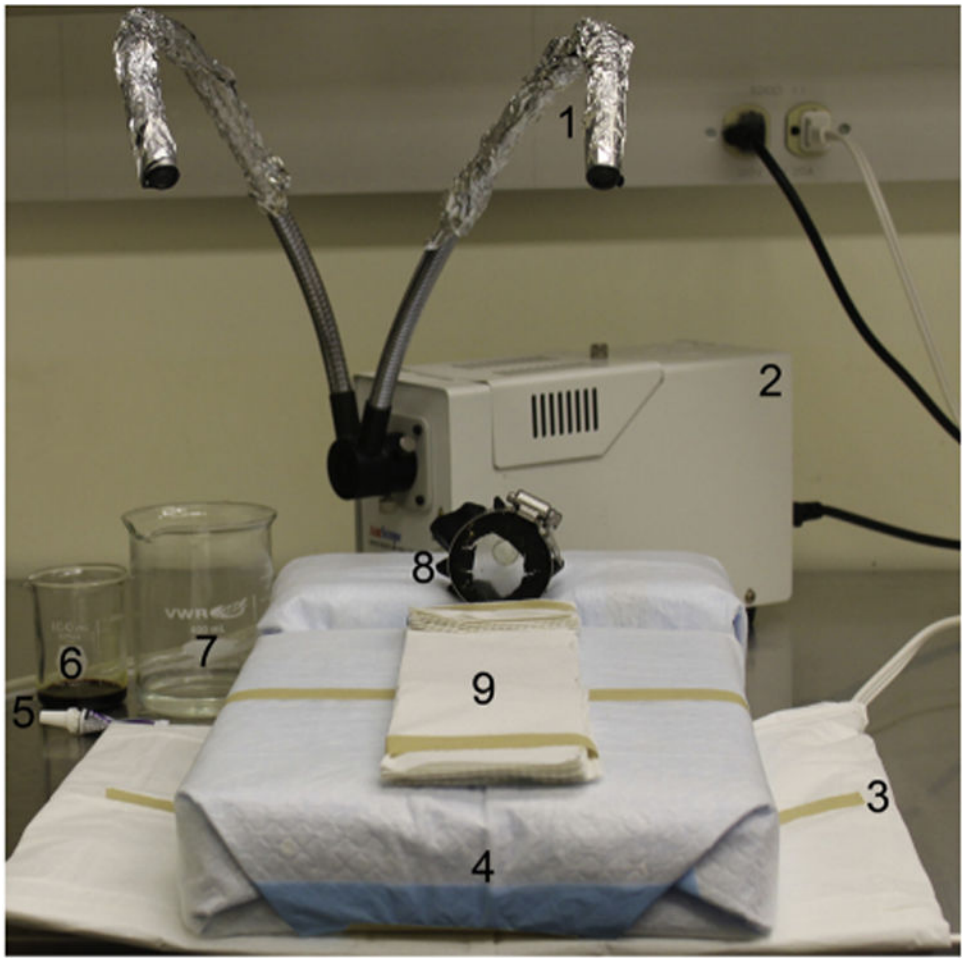

Fig 1.

Operative board setup: **(1)** sterile tinfoil, **(2)** light source, **(3)** heating pad, **(4)** operative board, **(5)** ocular lubrication, **(6)** Betadine (Purdue Pharma LP, Stamford, Conn), **(7)** alcohol, **(8)** nose cone, and **(9)** thermal insulation to protect from contact burns.

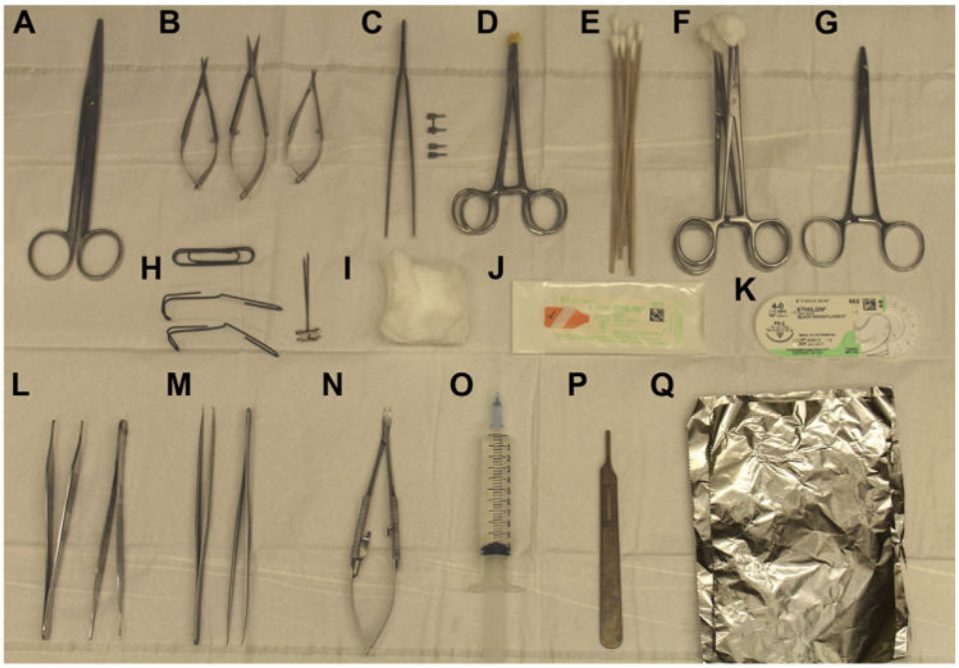

Fig 2.

Surgical instrument setup: **(A)** straight Mayo scissors, **(B)** Vannas spring scissors, **(C)** clamp applier with approximator clamp and single clamps, **(D)** rubber shods, **(E)** cotton swabs, **(F)** sponge on a stick, **(G)** needle driver, **(H)** retractors and pins, **(I)** sterile gauze, **(J)** 9-0 nylon suture, **(K)** 4-0 nylon suture, **(L)** smooth and toothed forceps, **(M)** 45° fine forceps, **(N)** Castroviejo needle driver, **(O)** heparinized saline, **(P)** ruler, and **(Q)** sterile tinfoil.

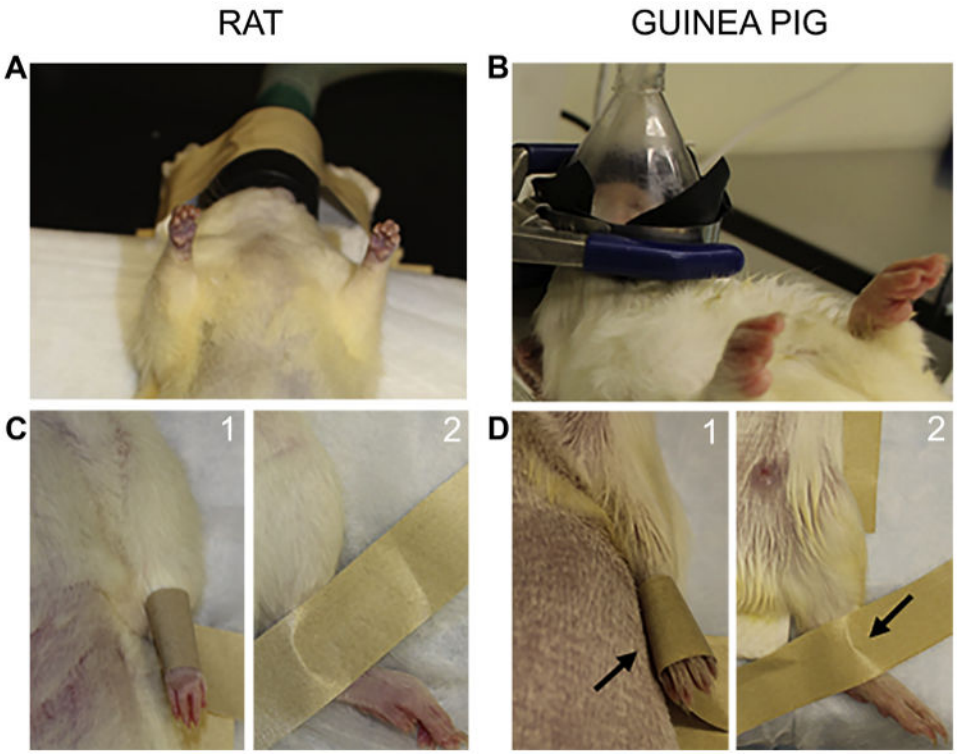

Fig 3.

Animal positioning. Positioning of the (**A**) rat and (**B**) guinea pig in the anesthetic nose cone. The guinea pig model required addition of a ring stand to suspend the nose cone and prevent hyperextension of the neck. Securing of the (**C**) rat and (**D**) guinea pig (**1**) forepaw and (**2**) hind paw to operative board (*arrow*).

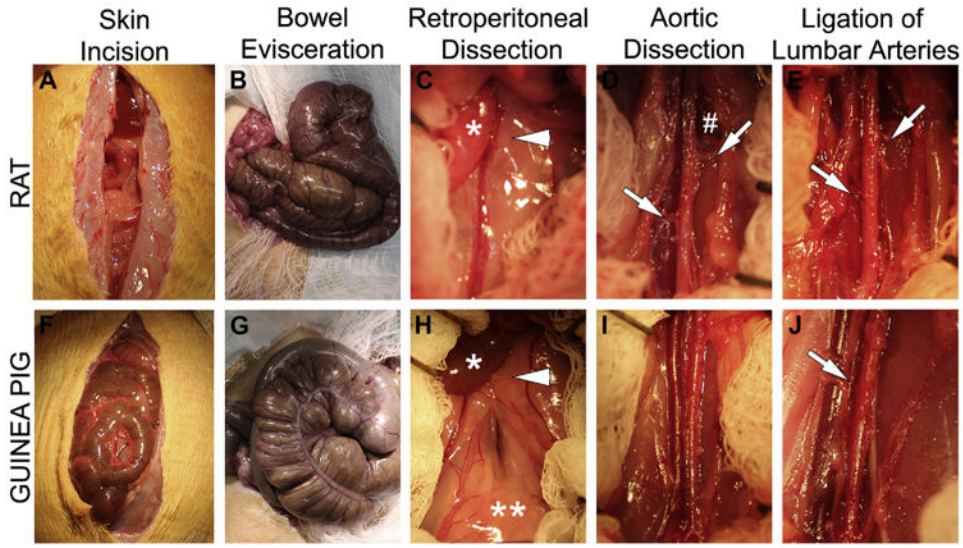

Fig 4.

Detailed operative approach to expose the abdominal aorta (**A-E**) in the rat and (**F-J**) guinea pig. Major steps include: abdominal incision, bowel evisceration, dissection of small bowel retroperitoneal attachments [*arrow head*], aortic dissection, and ligation of iliolumbar and lumbar arteries. **C** and **H**, The *arrowhead* indicates small-bowel retroperitoneal attachments; the * indicates small bowel; the ** indicates retroperitoneal fat. **D**, The # indicates the iliolumbar vein; the *arrows* indicate the right and left iliolumbar arteries. **E**, The *arrows* indicate the ligated right and left iliolumbar arteries. **J**, The *arrow* indicates the ligated lumbar artery.

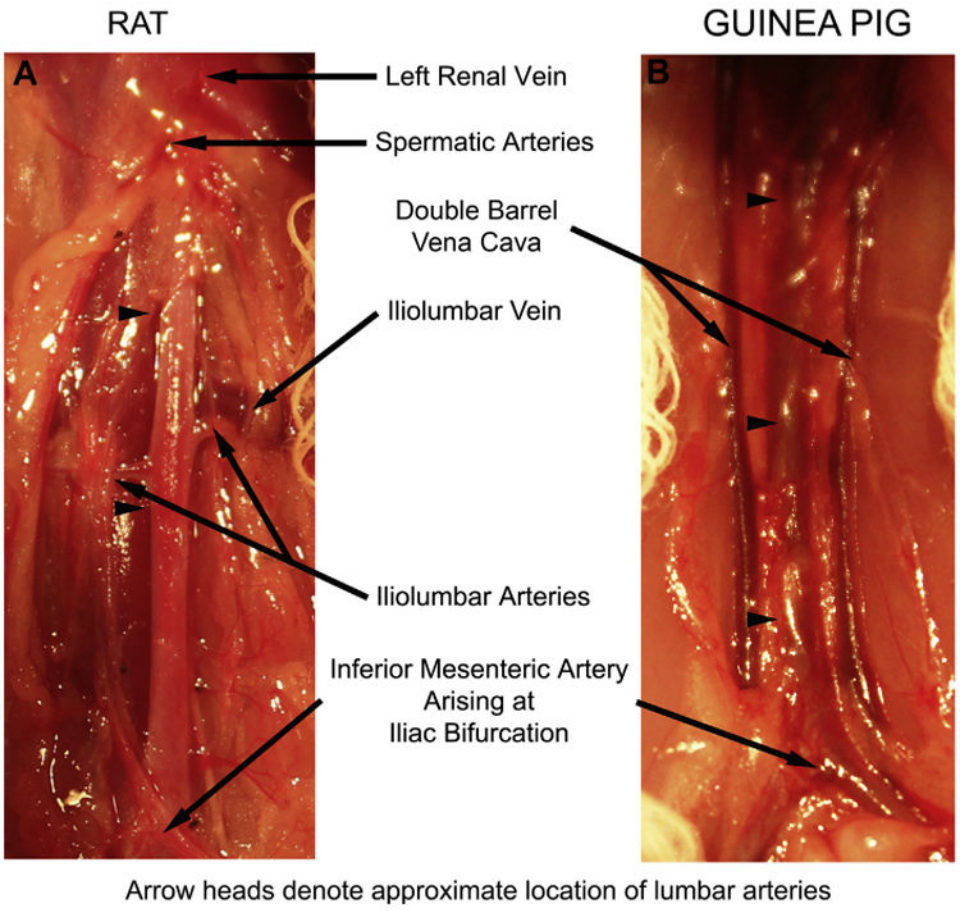

Fig 5.

Pertinent aortic anatomy of the (**A**) rat and (**B**) guinea pig. Limits of the dissection include the renal vein and spermatic arteries cranially and the inferior mesenteric arteries and bifurcation of the aorta into the iliac arteries caudally. The iliolumbar vein marks the location of the iliolumbar artery and the approximate locations of the five lumbar arteries that arise from the dorsal surface of the aorta. Branches ligated include the paired iliolumbar and proximal lumbar arteries in the rat and the lumbar arteries in the guinea pig. Note the common occurrence of a double-barrel inferior vena cava in the guinea pig. The *arrowheads* denote the approximate location of the lumbar arteries ligated in the (**A**) rat and (**B**) guinea pig.

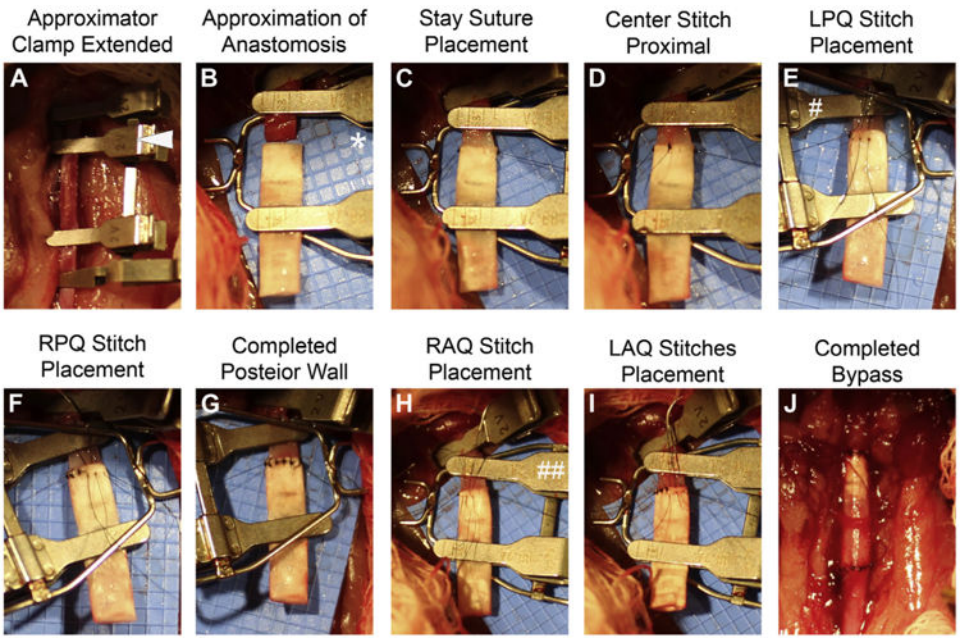

Fig 6.

A-J Detailed steps of the proximal anastomosis in the rat. The anastomosis is created with 12 interrupted sutures, including five in the posterior wall and five in the anterior wall. The distal anastomosis is created in a similar fashion. The same approach is used in the guinea pig model. The *arrowhead* denotes an extended approximator clamp; * indicates the blue visibility shield; # indicates approximator clamp rotated 180° counterclockwise; and ## indicates approximator clamp returned to neutral position. *LAQ*, Left anterior quadrant; *LPQ*, left posterior quadrant; *RAQ* right anterior quadrant; *RPQ*, right posterior quadrant.

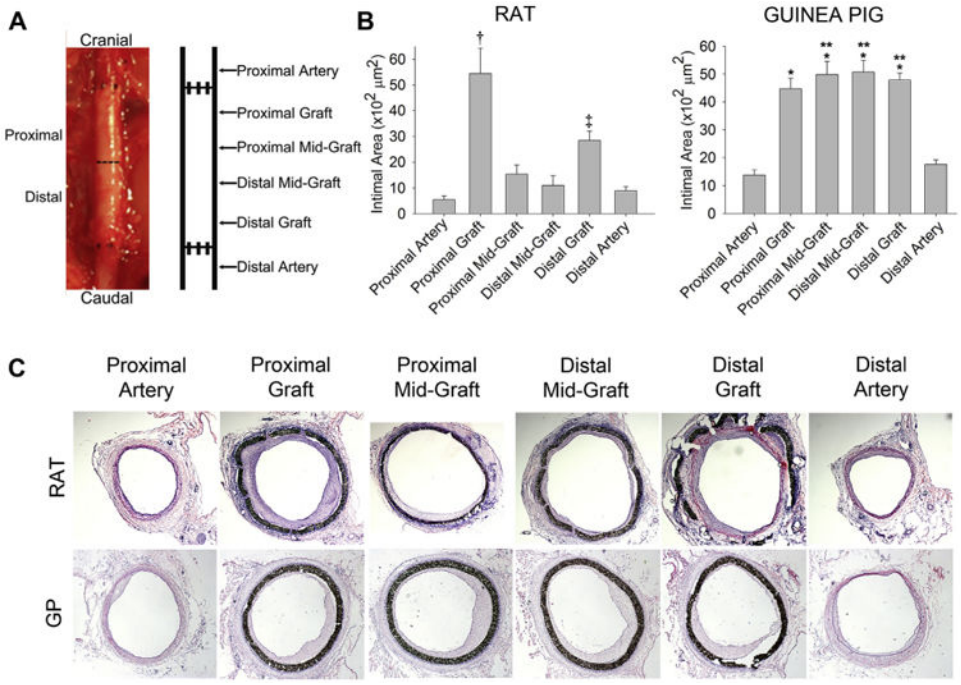

Fig 7.

Analysis of graft and artery intimal hyperplasia. **A**, Graft specimens explanted with 5 mm proximal and distal aorta 30 days after insertion were divided into proximal and distal segments, and intimal hyperplasia analyzed at six designated locations throughout the artery and graft. **B**, Intimal formation in the rat was greatest at the proximal graft ($^{\dagger}P < .001$ compared with the five other locations), followed by the distal graft ($^{\ddagger}P < .04$ compared with the proximal artery, distal midgraft, and distal artery). The guinea pig developed intimal hyperplasia similarly throughout the graft ($^{*}P < .001$ compared with the proximal and distal artery). Comparing the two animal models, the guinea pig developed more intimal hyperplasia at the proximal midgraft, distal midgraft, and distal graft compared with the rat at those similar locations ($^{**}P < .001$). The *range bars* show the standard error. **C**, Representative hematoxylin and eosin-stained cross sections (original magnification ×2.5) used for morphometric analysis.

Table I

Medications[a] commonly used with dosage information[b]

			Rat	Guinea pig		
Drug	**Class**	**Use**	**Range (Dose)**	**Range (Dose)**	**Benefits**	**Adverse effects**
Atropine	Anticholinergic	↓Mucus secretions	0.005-0.01 mg/kg[6] (0.01 mg/kg)	0.1-0.2 mg/kg[6] (0.1 mg/kg)	Cardioprotective	Urinary retention
Buprenorphine	Narcotic	Analgesia	0.01-0.05 mg/kg[7]	0.01-0.05 mg/kg[8]	Nonulcerogenic	↓Appetite, urinary retention
Carprofen	NSAID	Analgesia	5-10 mg/kg[7] (5 mg/kg)	2-4 mg/kg[9] (3 mg/kg)	Nonsedative analgesia	Ulcerogenic
Enrofloxacin	Fluoroquinolone	Infection prophylaxis	5-10 mg/kg[9] (5 mg/kg)	5-10 mg/kg[9] (5 mg/kg)	Broad-spectrum coverage	Diarrhea, renal toxicity
Heparin	Anticoagulant	Anticoagulant	(100 U/kg)[10]	(400 U/kg)[c]	Antithrombotic	Bleeding
Heparin Saline	Anticoagulant	Anticoagulant	100 U/mL	100 U/mL	Antithrombotic	Bleeding
Isoflurane	Halogenated anesthetic	Anesthetic	5% induction, then 2%-3%[9]	5% induction, then 1.5%-2.5%[9]	Easily titrated	No residual analgesia
Ketamine	NMDA antagonist	Anesthetic	60-70 mg/kg IP[7]	20-50 mg/kg IM[11]	↓Respiratory and cardiac depression	Not titratable, ↑secretions
Normal Saline	Replacement fluids	Hydration	100 mL/kg	100 mL/kg		
Ranitidine	H_2 blocker	GI prophylaxis	N/A	5-10 mg/kg[9] (5 mg/kg)	↓Gastric acid production	Arrhythmogenic (rare)

GI, Gastrointestinal; *IM*, intramuscular; *IP*, intraperitoneal; *N/A*, not applicable; *NMDA*, *N*-methyl-D-aspartate; *NSAID*, nonsteroidal anti-inflammatory drug.

[a] Medications are specified as generic drug name.

[b] Therapeutic ranges and dose used in the final model.

[c] Titrated to decrease early thrombosis rate.

Table II

Summary of the approaches used in the rat

First author, year	Anesthesia	Anticoagulation/ antiplatelet	Graft type, mm	Weeks implanted: Intima quantitated	Anastomotic technique: Aorta resected, mm	Anastomotic technique: Suture size type	Anastomotic technique: Stitch type, No.	Anastomotic technique: Anastomosis type/approach
Yeh,[14] 1984	Pentobarbital	Heparin IV	10	1-52	Yes	10-0	Interrupted	End-end
			HUA	No	3-4	Nylon	16	N/S
Ribbe,[15] 1987	Ether	Heparinized saline	PTFE	1-24	N/S	9-0 or 10-0	N/S	
			7 or 20	No	N/S	Nylon		Ligated iliolumbar/lumbar arteries
Lepidi,[16] 1996	Ketamine/xylazine		PTFE	4	N/S	10-0	N/S	End-end
			10	No	N/S	Nylon	N/S	N/S
Randone,[17] 1997	Ketamine/xylazine		Aorta	4	N/S	10-0	Continuous	End-end
			10	Yes	N/S	Nylon	N/S	N/S
Poston,[18] 1998	Methoxyflurane/pentobarbital	Heparinize graft	Aorta	2	N/S	8-0		End-side
				Yes	N/S	Polypropylene		Loop interposition
Dardik,[19] 1999	Methoxyflurane		PU	1-12	Yes	10-0	Interrupted	N/S
			10	Yes (Mid)	7	Nylon	N/S	
Jeschke,[20] 1999	Ketamine/xylazine		PU/ePTFE	1-4	N/S	-	N/S	N/S
			10	Yes (Avg Prox + Distal)	N/S	-	N/S	
Sterpetti,[21] 1999	Ketamine/xylazine		Aorta	4	N/S	10-0	Continuous	End-end
			10	Yes	N/S	Nylon	N/S	N/S
Andriambeloson,[22] 2001	$N_2O + O_2$/isoflurane		Aorta	2	N/S	N/S	N/S	End-end
			10	No	N/S			N/S
Johnson,[23] 2002	Pentobarbital		Aorta	8	N/S	9-0	N/S	End-end
			10	No	N/S	Nylon	N/S	
Kidd,[24] 2003	Pentobarbital		Aorta	8	N/S	9-0	N/S	End-end
			10	No	N/S	Nylon	N/S	
Yamamoto,[25] 2007	Pentobarbital	Heparin IV (100 U)	Femoral vein	1-4	N/S	10-0	Interrupted	End-end
			10	Yes (Prox, Dist, Mid)	N/S	Nylon	N/S	N/S
Cikirikcioglu,[26] 2008	Isoflurane	N/S	ePTFE	3	Beveled	10-0	Interrupted	End-end

				Weeks implanted	Anastomotic technique			
First author, year	**Anesthesia**	**Anticoagulation/ antiplatelet**	**Graft type, mm**	**Intima quantitated**	**Aorta resected, mm**	**Suture size type**	**Stitch type, No.**	**Anastomosis type/approach**
			20	No	15	Nylon	N/S	Ligated all side branches from renal artery to iliac bifurcation
Thaunat,[27] 2008	Pentobarbital	N/S	Aorta	2-13	N/S			End-end
			10	Yes	N/S			
Gui,[28] 2009	Ketamine/xylazine	Heparin (1000 IU/kg)/clopidogrel	Umbilical vein	2-8	N/S	10-0	N/S	
			8-10	Yes (Mid)	N/S	Nylon	N/S	
Pektok,[29] 2009	Isoflurane		ePTFE	3-24	Beveled	10-0	Interrupted	End-end
			10	Yes	10	Nylon		
Nieponice,[30] 2010	Isoflurane	Heparin IV (40 IU)	Tissue engineered	8	N/S	10-0	Interrupted	End-end
			10	No		Nylon		
Enomoto,[31] 2010	Pentobarbital	Heparin IV (100 IU/kg)	Silk fibroin	2-72	Yes	9-0	Interrupted	End-end
			10	No	10	Nylon	10-12	2 stay sutures 180°; front then back wall
Chen,[32] 2010	Pentobarbital	Graft heparinized	Femoral vein	24	N/S	8-0	Continuous	End-end
				Yes (aneurysmal site)	N/S	Polypropylene		
Ladhoff,[33] 2010	Ketamine/xylazine		Acellular aorta	2	N/S	8-0	N/S	End-end
				No	N/S	Nylon	N/S	
Thaunat,[34] 2010	Ketamine/xylazine	N/S	Aorta	4	N/S	N/S	N/S	End-end
			10	No	N/S	N/S	N/S	N/S
He,[35] 2010	Isoflurane/ketamine		PEUU	8		10-0		End-end
				No		Polypropylene		
Nakao,[36] 2011	Isoflurane		Vena cava	3	N/S			End-Side
			20	Yes				
Soletti,[37] 2011	Isoflurane/ketamine	Heparin IV (40 IU); aspirin (100 mg/kg/d)	PEUU	4-24	N/S	10-0	Interrupted	End-end
			10	No	N/S	Polypropylene	5-6	
Yagi,[38] 2011	Pentobarbital	Heparin IV (100 IU/kg)	Fibroin graft	2 and 8	Yes	9-0	Interrupted	End-end
			10	No	7	Nylon	8-10	
Sun,[39] 2012	Isoflurane		Vena cava	6	N/S			
			20	Yes	N/S			
Wu,[40] 2012	Isoflurane		PCL	2-13	Yes	9-0		End-end

				Weeks implanted	Anastomotic technique			
First author, year	**Anesthesia**	**Anticoagulation/ antiplatelet**	**Graft type, mm**	**Intima quantitated**	**Aorta resected, mm**	**Suture size type**	**Stitch type, No.**	**Anastomosis type/approach**
			8-10	No	4	Nylon		
Pennel,[41] 2013	Isoflurane	Heparin (1 mg/kg)	ePTFE + PU	2-6	N/S	9-0	Interrupted	End-end
			18.4/70.3	No	N/S	Nylon		
Kumar[42] 2013	Isoflurane	Heparinized graft	Collagen and elastin	2	Yes	10-0	Interrupted	
				No	5	8-10		
Dall'Olmo,[43] 2014	Isoflurane	N/S	Acellular	4-12	Yes	10	Continuous	End-end
			10	No	10	Polypropylene		

Dist, Distal; *ePTFE*, extended polytetrafluoroethylene; *HUA*, human umbilical artery; *IV*, intravenous; *Mid*, midgraft; *N/S*, not specified; *PCL*, poly(ɛ-caprolactone); *PEUU*, poly(ester urethane)urea; *Prox*, proximal; *PTFE*, polytetrafluoroethylene; *PU*, polyurethane.